Preliminary assessment of a novel small CSP plant based on linear collectors, ORC and direct thermal storage

Emiliano Casati[1,2], **Adriano Desideri**[3], **Francesco Casella**[4] **and Piero Colonna**[5]

[1] PhD candidate. Process and Energy Department, Delft University of Technology, Leeghwaterstraat 44, Delft-2628 CA, The Netherlands. Phone: +31152788254. E-Mail: e.i.m.casati@tudelft.nl

[2] PhD candidate. Dipartimento di Energia, Politecnico di Milano, Italy.

[3] MSc student. Process and Energy Department, Delft University of Technology, The Netherlands. Phone: +31683690858.

[4] Prof. Dr. Dipartimento di Elettronica e Informazione, Politecnico di Milano, Italy. Phone: +390223993465.

[5] Prof. Dr. Process and Energy Department, Delft University of Technology, The Netherlands. Phone: +31152782172.

Abstract

A novel power block for medium temperature concentrated solar power (CSP) applications based on the organic Rankine cycle (ORC) technology is presented in this paper, and its performance preliminary assessed through dynamic modelling tools. The main novelty is the integration in the plant's layout of a direct thermal energy storage (TES) system, which stores the same working fluid used in the power cycle. This allows for an unmatched simplification with respect to current state-of-the-art solutions, eliminating any intermediate heat transfer fluid (HTF) loop and its related components; however, in its simplest form, this concept yields to comparatively low storage densities. A practically feasible 100 kW_E case-study plant with 4 equivalent hours of thermal storage is presented. The proposed system exceeds 25% cycle's efficiency (air cooled with a condensing temperature of 80 °C) which, considering the coupling with parabolic trough collectors, yields 18% global system efficiency in design conditions. In order to investigate the control issues related to the proposed configuration, dynamic models have been developed for both the linear collectors and the TES system. These tools have been validated against literature data, and coupled to the recently developed model of a complete ORC unit, validated against proprietary experimental information. The possibility of ensuring safe automatic (and potentially unmanned) operations, while maintaining high conversion efficiency, is firstly assessed considering extreme conditions: the aspect of controllability is in fact considered of the utmost importance for the envisaged distributed applications.

1 Introduction

Recent studies have documented the potential of small-capacity CSP plants (up to 5000 kW_E), in case the future distributed energy scenario is considered [1]. The new envisaged development paradigm of "getting bigger by going smaller" could provide path to viability through modularity and economy of production, thus overcoming the bankability issue which is presently affecting this sector [2]. Furthermore, small-size CSP systems would be suitable for intercepting the emerging market opportunities in developing countries, with poor or non-existent power grid infrastructures [3].

The main advantage of CSP systems is the possibility of designing relatively cheap energy storage systems: comparing photovoltaic and CSP for large scale solar plants, the costs of storing energy can change the order of competitiveness in favour of the last [3, 4]. However, it is still not clear how this advantage could extend to the lower capacity-range, which would be of interest in a distributed production scenario.

In this context, an additional advantage of CSP plants could be the possibility of co-producing electricity and useful thermal outputs: of major interest is the coupling with heat-driven cooling systems, such as absorption chillers, to provide refrigeration power [5].

Among the technologies suitable for high-efficiency conversion of thermal power into electricity and heat in the range from few kW_E up to few MW_E, ORC turbogenerators stand out in terms of reliability and cost-effectiveness. ORC-based CSP plants have been widely studied, prototypes were put into operation several years ago [6, 7], and commercial plants went recently on-line [8].

To the knowledge of the authors, no research has been published on TES systems specifically conceived to be integrated into ORC power plants: however, thanks to the properties of commonly adopted ORC fluids, particularly efficient and simple TES concepts can be envisaged. A forthcoming publication deals in detail with this topic, illustrating how the concepts originally proposed for the direct storage of the working fluid in steam/water Rankine power plants [9] can be fruitfully extended to the ORC field [10].

In particular a fundamental plant's layout simplification is obtained, while preserving high levels of turnaround efficiency of the complete charge-standstill-discharge cycle: this is considered as a key point for the foreseen small-scale application. In the present work the developed preliminary design procedure is applied to a case-study plant, whose design performance are thus assessed.

Another aspect deemed crucial is the possibility of ensuring safe and efficient unmanned operations under all conditions, through automatic control procedures. A detailed dynamic model of the complete system is thus developed and applied, in order to investigate the control issues related to the proposed configuration.

2 System description

The ORC working fluid considered in this study is D_4(octamethylcyclotetrasiloxane, $C_6H_{24}O_4Si_4$), whose main properties are: molecular weight MW=296.6 kg/kmol; critical properties (temperature, pressure, and density): T_{CR}= 313.3 °C, p_{CR}= 13.32 bar, ρ_{CR}= 301.3 kg/m^3; normal boiling temperature T_{nb}= 175.3 °C. Siloxanes are silicon oils already employed in commercial high-temperature ORC applications since they are non-toxic, environmentally friendly, low-flammable, bulk produced and highly thermally stable; they are employed also as HTF in multiple fields, comprising the CSP industry [11, 12].

Multiparameter equations of state, in the Span-Wagner functional form, have been recently developed for these fluids [13]. Such thermodynamics models, implemented in the *Fluidprop* package [14], are adopted throughout this work.

The conceptual layout of a small-scale solar ORC power plant ($\dot{W}_{net}$ = 100 kW$_E$), featuring an highly integrated TES capable of 4 equivalent hours of storage[1], is shown in figure 1(a). The ORC working fluid is circulated and heated in the solar field (SF), which is composed of parabolic trough collectors with evacuated absorber tubes [15]; the same fluid serves also as the storage medium, making the concept completely direct. A single-vessel arrangement is chosen, relying on the thermocline effect in order to reduce exergy losses due to mixing of the cold and the hot fluid [16]: silicon oils have been already adopted in such applications [17]. Vapour generation is obtained through external flashing of the liquid extracted from the storage itself [9].

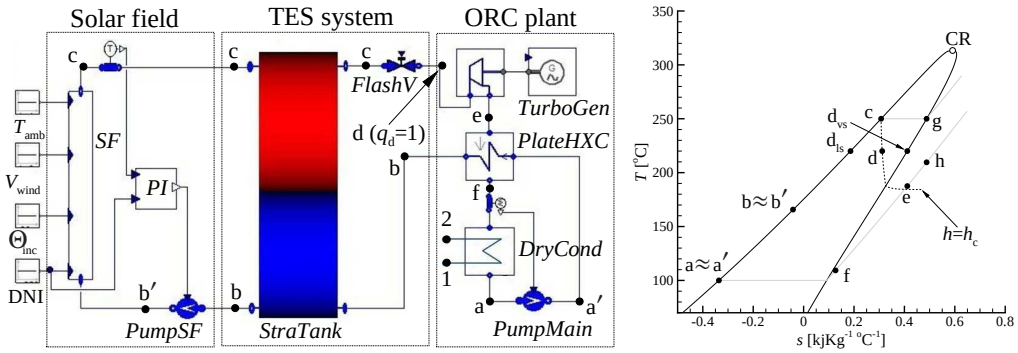

Figure 1: 1(a): simplified plant's layout of a CSP, ORC-based power system working according to the single-stage flash process, integrating a direct TES system based on a displacement type storage (from the Dymola-Modelica graphical user interface). 1(b): cycle state points in the $T-s$ chart of D_4. *CR*: liquid–vapour critical point, solid-black line: contour of the vapour-liquid equilibrium region, solid-grey: isobaric lines, dashed-black: iso-enthalpy line.

The design data adopted are reported in table 1: a relatively high value of the condensing temperature T_{cond} is chosen, which constitutes a major efficiency's burden. However, avoiding excessively low vacuum levels in the condenser is fundamental in high temperature applications, whereby the presence of air accelerates the working fluid's degradation. Realistic assumptions regarding both the dry air-cooled condenser and the plates-regenerator are considered: these have been derived from the preliminary design of the components, performed with a commercial package [18].

2.1 Working principle

In nominal conditions the temperatures at the outlet of the solar field $T_{out,SF}$, and in the hot region of the storage $T_{ST,hot}$ (which, in turn, equals that of the fluid fed to the ORC system), are considered to be both equal to T_c. This is chosen as the main operative variable (see sec. 2.2), while p_c is supposed to be maintained, through an external pressurizer, at a level higher (1 bar in design conditions) than the corresponding vapour pressure (being a single vessel, $p_c = p_b$).

[1]The size of the storage is usually expressed as equivalent hours of storage ($h_{eq,st}$): the corresponding thermal energy stored is the one needed to feed the power block at full load, for the same period of time.

Design data SF					
HCE	Schott PTR-70	SCA	ET-150	$\eta_{\text{opt,p}}$	0.75
DNI	850 [W/m^2]	Θ_{inc}	0 [°]	T_{amb}	30 [°C]
V_{wind}	0 [m/s]	$\Delta p_{\text{b'c}}$ 1 [bar]	SM	1.5	
Design data ORC					
$\dot{W}_{\text{E,net}}$	100 [kW$_{\text{E}}$]	Fluid	D_4	T_{cond}	80 [°C]
p_{cond}	0.035 [bar]	$\dot{m}_{\text{fluid}}$	1.81 [kg/s]	$\dot{m}_{\text{air}}$	8.61 [kg/s]
$T_{\text{c}} = T_{\text{out,SF}} = T_{\text{ST,hot}}$	312.6 [°C]	$p_{\text{c}} = p_{\text{ST}}$	14.2 [bar]	$h_{\text{eq,ST}}$	4 [hours]
$\Delta_{\text{pp,cond}}$	15 [°C]	ϵ_{reg}	0.85	$\eta_{\text{is,turbine}}$	0.85
$\eta_{\text{is,pumps-fans}}$	0.75	$\eta_{\text{M-E}}$	0.97	Δp_{ef}	50 [%p_{cond}]
Δp_{fa}	10 [%p_{cond}]	$\Delta p_{\text{a'b}}$	0 [bar]	Δp_{Fan}	5 [mm$_{\text{H}_2\text{O}}$]
Design performance					
η_{ORC}	0.251	$\eta_{\text{glob,SF}}$	0.71	$\eta_{\text{glob,sys}}$	0.178
A_{ap}	704 [m^2]	$\Delta \dot{V}_{\text{turb}}$	246	V_{ST}	65[m^3]
$m_{\text{fluid,ST}}$	$3E^4$ [kg]				

Table 1: Design data for steady-state modelling of the 100 kW$_{\text{E}}$ solar ORC. For a detailed description of the adopted heat collecting element (HCE) and solar collector assembly (SCA) technologies, see [19] and [20]. $\Delta p_{\text{b'c}}$: pressure drop in the SF, $\Delta_{\text{pp,cond}}$: pinch point temperature difference in the condenser, ϵ_{reg}: regenerator effectiveness, η_{is}: isoentropic efficiency, $\eta_{\text{M-E}}$: electro-mechanical efficiency of the generator and of all the electrical motors. Δp_{ef}, Δp_{fa}, $\Delta p_{\text{a'b}}$, and Δp_{Fan} : pressure drops in the regenerator (vapour side), in the condenser (process side), in the regenerator (liquid side), and in the condenser (static, air side) respectively.

Cold fluid is extracted from the vessel (*b*) and pumped through the SF: under normal operations the mass flow is controlled, acting on the pump, in order to maintain a given outlet temperature T_{c} (see sec. 4). Also in this case the temperature at the outlet of the regenerator $T_{\text{out,ORC}}$, and that of the cold fluid stored $T_{\text{ST,cold}}$, are considered equal to T_{b}.

The hot fluid extracted from the storage (*c*) is externally flashed to saturated vapour conditions, before feeding the ORC turbogenerator (*d*, with $q_{\text{d}} = 1$: see sec. 2.2). The superheated vapour leaving the turbine enters the regenerator (*e*), and then the condenser (*f*). The fluid, in saturated liquid conditions (*a*), is then pumped back, through the regenerator, to the bottom part of the storage vessel (*b*).

The mass flow circulating in the SF is determined by the available irradiation together with the collectors' area which, in turn, is related to the chosen solar multiple (SM)[2]. Optimal combinations of SM and size of the storage can be determined only through detailed techno-economic optimization procedures [21]: the values adopted here have therefore to be considered as purely indicative.

2.2 Flashing cycles with ORC fluids

In the proposed plant the storage system is *always on-line*, and the heat source and the power block are completely decoupled. As a consequence, the complete power system operates according to a thermodynamic cycle which includes a flashing evaporation process: such a "flashing cycle" (FC) is identified by the state points (fig. 1(b)) *a*, *b*, *c*, *d*, d_{vs}, *e*, *f* [22]. Being throttling a purely dissipative process, FCs have an inherently lower efficiency compared to the corresponding[3] evaporative ones (state points *a*, *b*, *c*, *g*, *h*, *f*) when evaluated for the exploitation of heat sources whose thermal capacity can be assumed infinite.

(chiarificare qui?) A FC allows nonetheless to avoid the need of evaporating the working fluid, either in the SF or in an additional evaporator, and makes feasible the complete decoupling of the heat source and the power block. Furthermore, as a consequence of the so-called retrograde behaviour of the considered fluids [23], the possibility exists of reaching complete vaporization during an isoenthalpic pressure-reduction (i.e. flashing). Such a FC, whereby the vapour quality is $q_{\text{d}} = 1$ (and $q_{\text{d}} \approx q_{\text{vs}}$), is designated here as a complete flashing cycle (CFC).

Adopting a CFC, which has not been considered before according to the authors' knowledge, makes redundant important components, such as the flashing vessel and the related liquid drains circuit: the flashing subsystem thus reduce to the throttling valve *FlashV* (see fig. 1(a)). All these features allows for a substantial simplification, both in terms of plant's layout and of operational procedures [24, 15].

[2] Defined as the ratio between the thermal power delivered by the actual SF under design irradiation, and the nominal thermal input to the power block.

[3] Is intended that the two cycles feature the same limiting temperature levels.

With complex siloxanes, operating at storage temperatures T_c close to the critical one, the implementation of a CFC does not imply severe efficiency losses with respect to the traditional EC solution: such a reduction could be accepted, considering the previously discussed advantages it allows for [10].

The choice of the working fluid and of the optimal $T_{c,R} \equiv T_c/T_{CR}$[4] then follows considerations related with other components: here the combination of D_4 and $T_{c,R} = 0.998$ is selected since it guarantees a comparatively high global (or solar-to-electric) efficiency $\eta_{glob,sys}$, while: i) maintaining the vacuum level in the low pressure part of the cycle in line with current ORC applications; ii) limiting the volumetric expansion ratio across the turbine $\Delta\dot{V}_{turb}$, such that it can be worked out with a comparatively simple machine [25].

The global efficiency is chosen as the key index of performance since it is directly related with the collectors' surface, which constitutes the main cost-driver in any CSP installation [26]. This quantity can be expressed as $\eta_{glob,sys} = \eta_{ORC} \cdot \eta_{glob,SF}$, where:

- $\eta_{ORC} = \dot{W}_{net}/\dot{Q}_{in,ORC}$ is the thermal efficiency of the ORC system. $\dot{W}_{net} = \dot{W}_{turbine} - \dot{W}_{aux}$ is the net electrical power delivered by the plant, after internal consumption for auxiliaries; $\dot{Q}_{in,ORC}$ is the thermal power supplied to the plant.

- $\eta_{glob,SF} = \dot{Q}_{in,ORC}/\dot{Q}_{av}$ is the global efficiency of the solar field, accounting for its optical and thermal efficiencies. $\dot{Q}_{av} = DNI_{des} \cdot A_{ap}$ is the thermal power made available from the sun's direct normal irradiation (DNI), at the given design value. The mirrors' aperture area A_{ap} can be evaluated as: $A_{ap} = \dot{W}_{net}/[\eta_{ORC} \cdot (q_{abs} - \dot{q}_{hl} - \dot{q}_{piping})]$: all the terms at the denominator represent thermal powers specific to the m^2 of mirrors' aperture area. $\dot{q}_{abs} = DNI_{des} \cdot \eta_{opt}$ is the thermal power absorbed by the collectors. Having assumed a null incidence angle for design calculations, the optical efficiency η_{opt} assumes its peak value $\eta_{opt,p}$ [27]. $\dot{q}_{piping}$ accounts for thermal losses in the piping subsystem of the SF, and a value of 10 [W/m^2] is assumed here [28]. $\dot{q}_{hl} = \mathcal{F}(T_{in,SF}, T_{out,SF}, \Theta_{inc}, V_{wind})$ accounts for the thermal efficiency of the solar absorbers, and is evaluated according to the detailed procedure presented in [20][5].

2.3 Results

The steady state modelling of the system is performed through an in-house *Matlab* code [29], coupled with *Fluidprop* for the accurate estimation of the fluids' thermophysical properties. The calculated performance are reported in table 1, while table 2 contains the cycle's state data points.

Table 2: Cycle state data points. Labels referring to the layout of fig. 1(a) and the $T - s$ diagram of fig. 1(b)

state	T °C	p [bar]	v [m^3/kg]	h [kj/kg]	s [kj/kg/K]	q [kg_{sv}/kg_{tot}]
a	80.0	0.035	0.001	-172.6	-0.43	0
b	205.6	14.197	0.001	59.1	0.12	-
c	312.7	14.197	0.002	291.8	0.56	-
d	283.2	8.486	0.011	291.8	0.57	1
e	234.9	0.057	2.489	233.6	0.59	-
f	87.6	0.039	2.551	4.5	0.07	-
1	30.1	1.001	0.880	0.0	-	-
2	67.0	1.000	1.052	37.2	-	-

Notwithstanding the chosen T_{cond}, the efficiency of the ORC power system exceeds 25% which, combined with the efficiency of the SF, yields a global efficiency in design conditions close to 18 %: this can be compared with the measured values for recently built state-of-the-art CSP plants (indirect system with synthetic oil as HTF and steam Rankine cycle), which are of the order of 22 % [30]. Even if no index of annual performance can be presently estimated, ORC power systems are characterized by better off-design behaviour if compared to steam cycles, and this is expected to partially overcome their lower design efficiency in an highly dynamic applications such as the CSP one.

The calculated values of storage density are lower than those characteristic of traditional TES solutions: the equivalent electrical energy density (EEED) of the stored liquid can be used as a term of comparison. The

[4] Here only the case of $T_{c,R} < 1$, i.e. storage of liquid, is considered.

[5] The coefficients adopted in the correlation proposed in the reference have been slightly modified, as a consequence of the different fluids and flow regimes, as discussed in [15].

proposed system approaches the limiting value of 6.2 [kWh_E/m^3_{ST}][6], while a recently designed displacement storage using synthetic oil as HTF, proposed to be coupled with the APS Saguaro ORC-based CSP plant [8], reaches approximately 15 [kWh_E/m^3_{ST}] [32]. This is mainly due to the low specific work extracted from the turbine, which causes the fluid to be injected back in the storage at a still high temperature ($T_b \equiv T_{out,ORC}$).

The need of a pressurized vessel further challenges the profitability of this solution; however, a detailed techno-economic analysis is needed in order to clarify this point.

3 Dynamic modelling

In order to study control issues related to the proposed configuration, dynamic models have been developed, using the *Modelica* object-oriented modelling language [33], for the linear collectors, the TES, and the ORC unit. All the needed fluid properties are computed with the *ExternalMedia* library [34] coupled to *Fluidprop* [14]. The simulations are performed with the commercial software Dymola [35].

3.1 Solar field

- The *SF* component models the solar field as it was composed by a single loop, whereby all the parabolic collectors are connected in series: this is modelled with a distributed parameters, finite volume approach. Each volume is implemented connecting 2 sub−components: the *Flow1D* model available from the *ThermoPower* library [36], and the newly developed *SolAbs* model.

  Flow1D models the working fluid's flow through the HCE, solving the 1D dynamic mass and energy balance equations, and the static momentum balance equation accounting for friction losses. The flow regime in the HCE is always turbulent, and the fluid-wall convective heat transfer coefficient U [$kW_T/m^2/°C$] is modelled, in off-design condition, according to the relation $U = U_{des} \cdot (\dot{m}_{fluid}/\dot{m}_{fluid,des})^{0.65}$.

  SolAbs, based on [28], models the dynamic 1D thermal energy balance on a HCE's cross section. It accounts for: conduction and storage in the metal pipe, convection and radiation in the vacuum chamber between the glass envelope and the metal pipe, conduction and storage in the glass envelope, convection and radiation transfers with the ambient air.
  Inputs to this model are the environmental parameters (*DNI*, Θ_{inc}, T_{amb}, and V_{wind}), and the fluid's inlet temperature from the *Flow1D* model. Output of *SolAbs* is the thermal power lost to the ambient $\dot{q}_{hl}$ (see sec. 2.2) and, consequently, the power transferred to the fluid which constitutes the input to *Flow1D*.

- The *PumpSF* component models the SF pump adopting a fictitious model, which imposes the flow rate passing through the machine (see also sec. 4), neglecting the fluid's specific enthalpy change across it. This follows the assumption that the dynamics of the recirculation pump is negligible compared to that of the solar collector.

  The complete solar collector model has been validated with reference data from [28].

3.2 Storage system

- The recently developed *StraTank* component models the thermocline storage with a 1D, first order finite volumes approach: the tank, supposed cylindrical, is discretized along its axis [37, 38]. A static momentum balance equation is implemented, which imposes a constant pressure in the tank (see sec. 2.1). Dynamic mass and energy balance equations are solved, accounting for the conductive heat transfer in the fluid and in the metal wall (along the vessel's height), and for the heat transfer between the wall and the fluid. Thermal energy storage in the metal wall is neglected, and three constant overall heat transfer coefficients are defined to model the thermal power lost to the environment from the roof, the foundation, and the wall of the tank.

  The four connecting flanges have a fixed position: the first volume to the top is linked to the outlet of the SF and to the inlet of the *FalshV*, and the last volume to the bottom is connected to the outlet of the regenerator and to the inlet of the SF pump. The turbulence mixing effects due to the introduction of fluid, on the stratification in the tank, are neglected. A trade-off exists in the selection of the number of discretization volumes: even though larger values lead to a more accurate evaluation of the transition

[6] This simplified approach assumes in fact that the storage delivers its full energy content without any variation in the discharged fluid's properties (conditions corresponding to state *c*). Thermal losses, as well as exergy losses due to deterioration of the stratification [31] are thus neglected: such simplifications are typically justified for daily charge-discharge cycles (relatively short standstill times).

zone, they also cause an underestimation of the dumping effect introduced by the storage between the variations of the inlet ($T_{\text{out,SF}}$) and the outlet ($T_{\text{ST,hot}}$) temperatures.

The *StraTank* model has been validated based on experimental data from the open literature [38].

- The *FlashV* component models the throttling valve which realizes the flashing process (see sec. 2.2). It is a model that trivially represents an ideal control acting on the valve's opening, able to assure flashing down to saturated vapour conditions: given the storage conditions, and modelling the process in the valve as an isoenthalpic pressure reduction, an outlet pressure p_{d} is imposed such that $p_{\text{d}} = p(h_{\text{ST,hot}}, q = 1)$

3.3 ORC power block

- The *TurboGen* component is implemented connecting the recently developed *ChockTurb* model [39], and the *ElecGen* model from *ThermoPower*.

  ChockTurb models a supersonic axial turbine as a *de Laval* nozzle, assumed to be chocked in all operating conditions. The result of the design calculation is the critical nozzle area (where sonic conditions occur) and, for off-design conditions, the relation between mass flow and inlet pressure is implemented (considering isoentropic expansion). *ElecGen* trivially models the electrical generator, without accounting for any dynamics.

  Both the the turbine's isoentropic efficiency, and the generator's electro-mechanical efficiency, are considered constant.

- The *PlateHXC* component models a counter−current plate heat exchanger: it is implemented connecting different sub−models from [36]: two *Flow1D* components, representing the fluid's flow in the two sides of the exchanger (see sec. 3.1), two *ConvHT* components modelling the convective heat transfer between the two streams and the interposed metal wall, and a *MetalWall* component modelling the heat conduction and the storage of energy in the wall itself.

- The *DryCond* component models a dry air-cooled condenser: assuming that the cooling fans are controlled in order to maintain the condensing pressure close to the design value, a trivial model is implemented. This imposes both the pressure and temperature on the main pump's side, and the pressure at the regenerator's side. Introducing this simplification, an increased robustness for the whole plant's model, and a decrease in the computational time, are achieved.

- The *PumpMain* component is equivalent to *PumpSF* (see sec. 3.1). In this case the circulating mass flow rate imposed to the pump is determined by the *ChockTurb* model.

  The complete model of the ORC power block has been validated with field data collected during a recent measurement campaign [39].

4 Control strategy

As anticipated in section 3, both the *FlashV* (sec. 3.2) and the *DryCond* models incorporate "perfect controllers" which made them able to exactly accomplish the imposed tasks. This simplified approach, which avoid the need of a detailed modelling of the complete control scheme, is deemed satisfactory for the scope of the present work, whereby only the main control loop related to the SF dynamics is of interest.

For this subsystem, the control strategy selected in this preliminary study aims at keeping the temperature at the outlet of the SF $T_{\text{out,SF}}$ close to the nominal value under transient conditions: even though this is known to be a sub-optimal solution [40], it is nonetheless of relatively simpler implementation and interpretation.

The regulator is of the proportional-integer (PI) type: the controlled variable is $T_{\text{out,SF}}$, and the control variable is the pump's rotational speed which varies the mass flow flowing in the SF.
The PI regulator has been calibrated considering a transfer function based on the following concentrated parameters model of the solar collector: $T(x)/dx = (T_{\text{out,SF}} - T_{\text{in,SF}})/L_{\text{SF}}$ where L_{SF} is the total length of the collectors' loop.
The changes in *DNI* are supposed to be measured: a direct compensation of such disturbances it has been thus implemented in the controller in order to anticipate their effects. The parameters of the regulator (proportional gain k_{p} and integral time T_{I}) have been chosen in order to obtain a critical pulse equal to $\omega_c = 2 \cdot \tau^{-1}$, where τ is the time needed, for the fluid in nominal conditions, to pass through the solar field. The controller signal has been saturated in order to prevent sharp changes of the *DNI* from causing stresses to the centrifugal pump: the

regulator saturates at 0.1 and 4.5 kg/s; the pump dynamics has been considered by adding a constant time delay of 15 seconds.

5 Dynamic simulation and results

The complete model introduced in sec.3, and controlled according to the scheme described in sec.4, is used to study the dynamic performance of the case-study plant proposed in sec.2.
As anticipated, the main scope is to assess if the whole system can be safely and efficiently operated through automatic control procedures.

From the safety point of view, the main concern regards the possibility of thermal decomposition of the working fluid to occur: for D_4 the limit is around 400°C $=T_{max}$ [11].
Due to the favourable properties of silicon oils, the corresponding heat transfer coefficient is large enough to prevent, under all the foreseeable operating conditions, the wall temperature to exceed T_{max} [15].
However, as a consequence of the adopted control strategy, a drop in the mass flow circulating in the SF follows a reduction of the solar input (*DNI*): a subsequent sharp increase in the *DNI* may cause, if the system's reaction is not fast enough in increasing the mass flow again, the limit of T_{max} to be reached.

From the efficiency point of view, keeping $T_{out,SF}$ always close to the nominal value allows to preserve the stratification in the storage vessel: the turnaround efficiency of the TES system is consequently increased. In fact, being $T_{ST,hot}$ the temperature of the fluid fed to ORC system, maintaining it as close as possible to the nominal value allows the power block to be operated in conditions close to the design ones for a larger number of hours.

The virtual plant is thus tested under a situation representative of extreme working conditions [41], whereby a series of clouds (3 in this example) causes the solar input to periodically drop, and than sharply return to the nominal value. This effect is modelled applying a signal with subsequent ramps to the *DNI* input of the SF model (see fig. 2)[7]: the *DNI* is supposed to drop down to 10 % of its nominal value, perturbing the initial steady state condition (design point, storage fully charged).

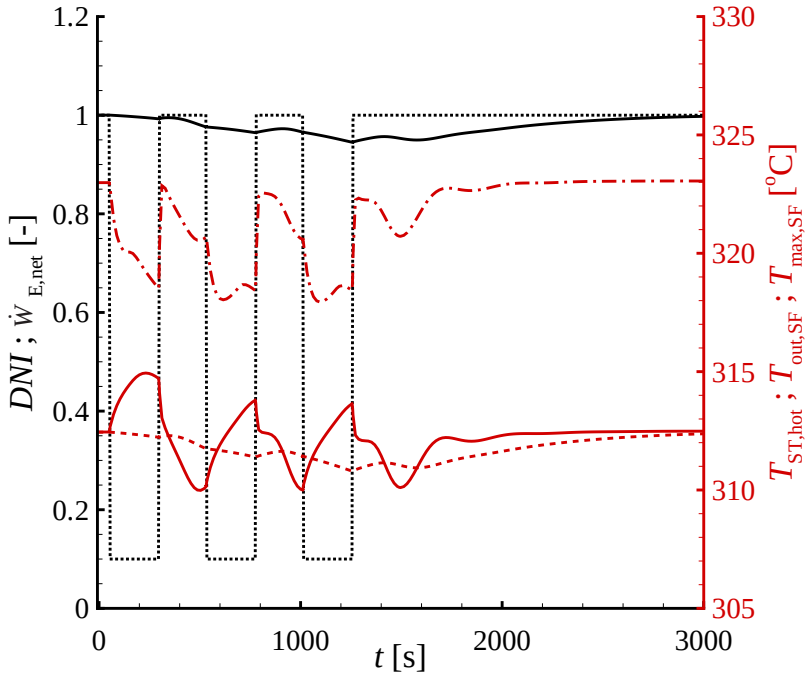

Figure 2: Dynamic simulations results, for the virtual solar ORC plant, under time-varying solar input. The black dotted line represents the non dimensional *DNI* (w/r to its nominal value): it drops to 10 % in 5 s, remains constant for 4 mins (240 s), and then sharply returns to its nominal value (in 5 s); the interval between two subsequent drops is approximately 4 mins (230 s). Black solid line: $\dot{W}_{E,net}$; red solid line: $T_{out,SF}$; red dashed line: $T_{ST,hot}$; red dash-dotted line: $T_{max,SF}$.

[7] The clouds are therefore supposed to "uniformly shading" the complete SF.

From the results collected in figure 2, appears that the virtual plant is characterized by time constants which are large enough to lead to an overlapping effect of the disturbances, as already noted in previous works [41].

The ability of the control system to maintain $T_{\text{out,SF}}$ close to its nominal value is proved: the maximum predicted range of oscillation around the design value is 5 °C.

Also the maximum temperature in the solar field $T_{\text{max,SF}}$, which occurs in the last segment of the discretized collector for all the simulated conditions, remains within safe values and, in particular, is always lower than its design value.

Also the effectiveness of the TES system in decoupling the ORC power block from the SF is assessed: the oscillations in $T_{\text{ST,hot}}$ (corresponding to the turbine inlet temperature) are in fact substantially dumped with respect to those in $T_{\text{out,SF}}$: a maximum difference of less than 2 °C is predicted. As a consequence, the maximum drop in the delivered power $\dot{W}_{\text{E,net}}$ is about 5.5%.

6 Conclusions

A novel power block for small-capacity, medium-concentration CSP applications, based on the ORC technology, is presented in this work. The main novelty is constituted by the TES system, which adopts the same working fluid as storage medium, and completely decouples the solar field from the power block. As a consequence, an unmatched simplification both in terms of plant's layout and of operational procedures is achieved.

This is made possible by the adoption of the newly introduced thermodynamic cycle named CFC (Complete Flashing Cycle), featuring a flashing evaporation process of the working fluid, from the conditions of the stored liquid down to those of the saturated vapour entering the turbine.

The presented 100 kW_Ecase-study plant, adopting D_4as the working fluid, achieves a solar-to-electric efficiency of 18% in design conditions. A dynamic model, developed and validated for the complete system, is used to investigate the performance under extreme transient conditions: the feasibility of remotely controlled operation is thus preliminary assessed.

The comparatively low storage densities, and high cost of silicon oils, together with the adoption of a pressurized vessel, are likely to penalize the direct storage of ORC fluid in its simplest form presented here: a detailed techno-economic analysis, needed to evaluate the profitability of the proposed solution, will be developed as the next step of this work.

citare sistema binario come possibile via per aumentare le prestazioni ??

References

[1] E. Prabhu, "Solar trough organic rankine electricity system (STORES) stage 1: Power plant optimization and economics," Tech. Rep. NREL/SR-550-39433, National Renewable Energy Laboratory, 2006.

[2] A. Skumanich, "CSP at a crossroads: The first solar electric power plants are still proving their worth after three decades, so why aren't we seeing more csp reach the development stage?," *Renewable Energy Focus*, vol. 12, no. 1, pp. 52–55, 2011.

[3] M. Peters, T. Schmidt, D. Wiederkehr, and M. Schneider, "Shedding light on solar technologies-a techno-economic assessment and its policy implications," *Energy Policy*, vol. 39, no. 10, pp. 6422–6439, 2011.

[4] ESTELA, "Solar thermal electricity 2025. clean electricity on demand: attractive ste cost stabilize energy production.," tech. rep., 2010.

[5] F. Al-Sulaiman, F. Hamdullahpur, and I. Dincer, "Trigeneration: A comprehensive review based on prime movers," *International Journal of Energy Research*, vol. 35, no. 3, pp. 233–258, 2011.

[6] H. Tabor and L. Bronicki, "Establishing criteria for fluids for small vapor turbines," in *SAE National Transportation, Powerplant, and Fuels and Lubricants Meeting*, October 1964.

[7] G. Angelino, M. Gaia, and E. Macchi, "Review of italian activity in the field of organic rankine cycles.," in *Proceedings of the International VDI-Seminar on ORC-HP-Technology*, pp. 465–482, VDI Verlag, Duesseldorf, 1984.

[8] S. Canada, D. Brosseau, and H. Price, "Design and construction of the APS 1-MW_E parabolic trough power plant," in *Proceedings of the ASME International Solar Energy Conference 2006*, vol. 2006, (Denver, CO), 2006.

[9] G. Beckam and P. Gilli, *Thermal Energy Storage*. Springer–Verlag, 1984.

[10] E. Casati, A. Galli, and P. Colonna, "Direct working fluid storage for ORC power systems," 2012. Submitted for publication.

[11] G. Angelino and C. Invernizzi, "Cyclic methylsiloxanes as working fluids for space power cycles," *Journal of Solar Energy Engineering, Transactions of the ASME*, vol. 115, no. 3, pp. 130–137, 1993.

[12] DOW, "SYLTHERM 800 Heat Transfer Fluid - Product Technical Data," tech. rep., Dow Corning Corporation, 2012.

[13] P. Colonna, N. R. Nannan, A. Guardone, and E. W. Lemmon, "Multiparameter equations of state for selected siloxanes," *Fluid Phase Equilibria*, vol. 244, no. 2, pp. 193–211, 2006.

[14] P. Colonna and T. P. van der Stelt, "Fluidprop: a program for the estimation of thermophysical properties of fluids. available from www.fluidprop.com," tech. rep., Delft Technical University of Technology, 2004.

[15] E. Casati, P. Colonna, and N. R. Nannan, "Supercritical ORC turbogenerators coupled with linear solar collectors," in *Proceedings of the ISES Solar World Congress 2011*, (Kassel), 28 Aug.-2 Sept. 2011.

[16] A. M. Kandari, "Thermal stratification in hot storage-tanks," *Applied Energy*, vol. 35, no. 4, pp. 299 – 315, 1990.

[17] A. Gil, M. Medrano, I. Martorell, A. Lzaro, P. Dolado, B. Zalba, and L. Cabeza, "State of the art on high temperature thermal energy storage for power generation. part 1-concepts, materials and modellization," *Renewable and Sustainable Energy Reviews*, vol. 14, no. 1, pp. 31–55, 2010.

[18] Aspen Technology Inc., *Exchanger Design and Rating, ver. 7.2*. 2007. http://www.aspentech.com.

[19] A. Fernández-García, E. Zarza, L. Valenzuela, and M. Pérez, "Parabolic-trough solar collectors and their applications," *Renewable and Sustainable Energy Reviews*, vol. 14, no. 7, pp. 1695–1721, 2010.

[20] F. Burkholder and C. Kutscher, "Heat loss testing of schott's 2008 ptr70 parabolic trough receiver," Tech. Rep. NREL/TP-550-45633, National Renewable Energy Laboratory, 2009.

[21] J. Cabello, J. Cejudo, M. Luque, F. Ruiz, K. Deb, and R. Tewari, "Optimization of the size of a solar thermal electricity plant by means of genetic algorithms," *Renewable Energy*, vol. 36, no. 11, pp. 3146 – 3153, 2011.

[22] T. Ho, S. Mao, and R. Greif, "Comparison of the organic flash cycle (OFC) to other advanced vapor cycles for intermediate and high temperature waste heat reclamation and solar thermal energy," *Energy*, vol. 42, no. 1, pp. 213 – 223, 2012.

[23] P. Colonna and A. Guardone, "Molecular interpretation of nonclassical gas dynamics of dense vapors under the van der waals model," *Physics of Fluids*, vol. 18, no. 5, 2006.

[24] L. Valenzuela, E. Zarza, M. Berenguel, and E. Camacho, "Control concepts for direct steam generation in parabolic troughs," *Solar Energy*, vol. 78, no. 2, pp. 301–311, 2005.

[25] A. Verneau, "Application of organic fluids in solar turbines [l'emploi des fluides organiques dans les turbines solaires]," *Entropie*, vol. 14, no. 82, pp. 9–18, 1978.

[26] R. Pitz-Paal, J. Dersch, B. Milow, F. Téllez, A. Fernere, U. Langnickel, A. Steinfeld, J. Karni, E. Zarza, and O. Popel, "Development steps for parabolic trough solar power technologies with maximum impact on cost reduction," *Journal of Solar Energy Engineering, Transactions of the ASME*, vol. 129, no. 4, pp. 371–377, 2007.

[27] J. Duffie and W. Beckam, *Solar Engineering of Thermal Processes*. John Wiley & Sons, Inc., 3^{rd} ed., 2006.

[28] R. Forristall, "Heat transfer analysis and modeling of a parabolic trough solar receiver implemented in engineering equation solver," Tech. Rep. NREL/TP-550-34169, National Renewable Energy Laboratory, october 2003.

[29] The MathWorks Inc., *Matlab, ver. 7.13.0.564*. 2011. www.themathworks.com.

[30] A. Giostri, M. Binotti, M. Astolfi, P. Silva, E. Macchi, and G. Manzolini, "Comparison of different solar plants based on parabolic trough technology," *Solar Energy*, vol. 86, no. 5, pp. 1208–1221, 2012.

[31] M. Haller, E. Yazdanshenas, E. Andersen, C. Bales, W. Streicher, and S. Furbo, "A method to determine stratification efficiency of thermal energy storage processes independently from storage heat losses," *Solar Energy*, vol. 84, no. 6, pp. 997–1007, 2010.

[32] G. Kolb and V. Hassani, "Performance analysis of thermocline energy storage proposed for the 1 MW saguaro solar trough plant," in *Proceedings of the ASME International Solar Energy Conference*, vol. 2006, (Denver, CO), 2006.

[33] Website, "< *www.modelica.org* >,"

[34] F. Casella and C. Ritcher, "ExternalMedia: a library for easy re-use of external fluid property code in Modelica," in *Proceeding of the 6th International Modelica Conference* (B. Bachmann, ed.), Modelica Association, 2008.

[35] Website, "< *www.dynasim.se* >,"

[36] F. Casella and A. Leva, "Modelica open library for power plant simulation: design and experimental validation," in *Proceedings of the 3rd International Modelica Conference* (P. Fritzson, ed.), Modelica Association, 2003.

[37] A. Galli, "Assessment of direcct working fluid storage concepts for orc power systems," Master's thesis, Politecnico di Milano, 2012.

[38] Y. Zurigat, K. Maloney, and A. Ghajar, "Comparison study of one-dimensional models for stratified thermal storage tanks," *Journal of Solar Energy Engineering, Transactions of the ASME*, vol. 111, no. 3, pp. 204–210, 1989.

[39] F. Casella, T. Mathijssen, P. Colonna, and J. van Buijtenen, "Dynamic modeling of orc power systems," 2012. Submitted for publication.

[40] A. Bejan, "Extraction of exergy from solar collectors under time-varying conditions.," *Int. J. Heat & Fluid Flow*, vol. 3, no. 2, p. Bejan1981, 1981.

[41] M. Eck and T. Hirsch, "Dynamics and control of parabolic trough collector loops with direct steam generation," *Journal of Solar Energy*, vol. 81, pp. 268–279, 2006.